Advanced Physical Research
Vol.5, No.3, 2023, pp.168-176

SIMULATION OF THE ELECTROMAGNETIC FIELD OF A MICROWAVE WAVEGUIDE TAKING INTO ACCOUNT THE ANISOTROPY OF THE MEDIUM

I.J. Islamov*, I.A. Aslanzadeh

Azerbaijan Technical University, Baku, Azerbaijan

Abstract. In this work, the simulation of the electromagnetic field of the microwave waveguide is carried out, taking into account the anisotropy of the medium. A dispersion equation and expressions for the reflection and transmission coefficients of a waveguide wave are obtained. 3*D* radiation patterns of the microwave range waveguide are plotted taking into account the gyrotropy of the medium. On the basis of the developed new method, an explicit analytical solution of the boundary value problem of natural and forced oscillations of a ferrite resonator in a microwave rectangular waveguide with a transverse magnetic field is found. Various modes of excitation of bulk and surface self-oscillations in a ferrite resonator are analyzed.

Keywords: *Resonator, electromagnetic field, rectangular waveguide, modeling, signals, transmission lines.*

****Corresponding Author:*** *I.J. Islamov, Azerbaijan Technical University, H. Javid ave. 25, AZ-1073, Baku, Azerbaijan, Tel.: +994 50 626 76 99, e-mail: icislamov@mail.ru; icislamov@aztu.edu.az*

Received: *15 June 2023;* ***Accepted:*** *29 July 2023;* ***Published:*** *03 October 2023.*

1. Introduction

Ferrite resonators are widely used in passive and active devices of the microwave terahertz wavelength range to electrically control their output characteristics. Among the vase elements of devices is its simplest form of a rectangular resonator placed in a rectangular waveguide with a transverse magnetic field. This design can act as a controlled frequency filter and be used, for example, as a waveguide window for active electronic devices. Naturally, for a complete understanding of the physics of processes in such a microwave device, it is necessary to solve the corresponding electrodynamic problem on natural or forced oscillations of such a device. Until recently (Kerim *et al*., 2015; Taisir *et al*., 2010; Wang *et al*., 2018), when calculating such resonators, as a rule, numerical methods (Lima *et al*., 2021; Lima *et al*., 2020; Li *et al*., 2020; Liang *et al*., 2017) were used based on systems of linear algebraic equations for the unknown coefficients of the Fourier expansion of fields in the partial domain method. The analytical solution was obtained in the one-wave approximation. In (Singh *et al*., 2020; Yang *et al*., 2021; Wang *et al*., 2019; Hui *et al*., 2022), a new approach was proposed for finding an analytical solution to a boundary value problem based on the theory of entire analytic functions, the theory of residues, and the Lagrange interpolation formula. As a result of applying this approach, it was possible to solve analytically a system of linear

How to cite (APA):
Islamov, I.J., Aslanzadeh, I.A. (2023). Simulation of the electromagnetic field of a microwave waveguide taking into account the anisotropy of the medium. *Advanced Physical Research, 5*(3), 168-176.

algebraic equations in closed form for arbitrary parameters of the problem and to find in an analytical form the dispersion equation for finding the eigen modes of a ferrite resonator in a waveguide, as well as to obtain simple expressions for the reflection and transmission coefficients of the waveguide wave.

2. Statement and solution of the problem

A two-dimensional model of a ferrite resonator is considered (Figure 1).

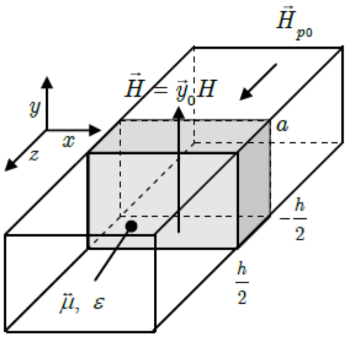

Fig. 1. Ferrite resonator in the waveguide with transverse magnetic field $\vec{H} = \vec{y}_0 H$

The magnetic permeability of ferrite is described by a tensor of the standard type. The tensor elements depend on the applied magnetic field and the signal frequency according to the well-known formulas (Castillo *et al*., 2021; Liu *et al*., 2019; Islamov *et al*., 2018; 2019):

$$\vec{\mu} = \begin{Vmatrix} \mu & -i\mu_a & 0 \\ i\mu_a & \mu & 0 \\ 0 & 0 & 1 \end{Vmatrix},$$

where $\mu = \dfrac{\omega_H(\omega_H + \omega_M)}{\omega_H + \omega^2}$; $\mu_a = \dfrac{\omega\omega_M}{\omega_H - \omega^2}$; $\omega_M = \gamma 4\pi M_0$; $\omega_H = \gamma H_0$.

To find natural and forced vibrations in a ferrite resonator, it is necessary to solve the boundary electrodynamic problem with the corresponding boundary conditions on the surfaces of the resonator. For a given configuration of a resonator with a transverse magnetic field, such a problem is reduced to finding a solution to the Helmholtz equation with respect to the field component E_z, namely:

$$\frac{\partial^2 E_z}{\partial y^2} + \frac{\partial^2 E_z}{\partial x^2} + k^2 \varepsilon \mu_\perp E_z = 0, \tag{1}$$

where $\mu_\perp = \mu\left(1 - \dfrac{\mu_a^2}{\mu^2}\right)$, $\varepsilon -$ dielectric constant of a gyromagnetic medium, $k = \dfrac{2\pi}{\lambda}$.

To find forced vibrations, it is necessary to consider the problem of diffraction of a waveguide won by a ferrite resonator. The natural oscillations are determined from the solution of the problem in the absence of the incident wave. Using the Fourier method in combination with the partial domain method, we write down the solutions of the Helmholtz equation in the form (Ismibayli *et al*., 2018; Islamov *et al*., 2019; 2022):

$$E_z^1 = \sin\frac{\pi p}{b} y e^{+i\gamma_p \omega} + \sum_{n=1} R_n e^{-i\gamma_n \omega} \sin\frac{\pi n}{b} y, \tag{2}$$

$$E_z^2 = \sum_{n=1}\left(D_n^+ e^{i\chi_{na}\omega} + D_n^- e^{-i\chi_{na}\omega}\right)\sin\frac{\pi n}{a} y, \tag{3}$$

$$E_z^3 = \sum_{n=1} T_n e^{i\gamma_n \omega} \sin\frac{\pi n}{b} yp, \tag{4}$$

where $\gamma_n^2 = k^2 - \left(\frac{\pi n}{a}\right)^2, \chi_{na}^2 = k^2 \varepsilon \mu_\perp - \left(\frac{\pi n}{a}\right)^2.$

The tangential components of the magnetic field are determined from Maxwell's equations by the formula

$$H_\omega = -\left(\frac{1}{ik\mu_\perp}\right)^2 \left(\frac{\partial E_y}{\partial z} - i\frac{\mu_a}{\mu}\frac{\partial E_y}{\partial x}\right)^2. \tag{5}$$

Using the boundary conditions on the resonator surfaces, one can obtain a coupled system of two systems of linear algebraic equations to determine the unknown coefficients (2)-(4)

$$W_m^{\mp} X_m^{\pm} - \frac{\mu_a}{\mu}\sum_{n=1}^{\infty} X_n^{\mp}\left(\frac{\pi m}{a}\right) L_{nm} = \mu_\perp \gamma_p e^{-i\gamma_p \frac{h}{2}} \delta_{mp}, \tag{6}$$

where $2X_n^{\pm} = (R_n \pm T_n) e^{i\gamma_n \frac{h}{2}} + \delta_{np} e^{i\gamma_n \frac{h}{2}}$, $L_{nm} = -\sin\pi\frac{(n-m)}{2}\frac{\sin\pi\frac{(n-m)}{2}}{\pi\frac{(n-m)}{2}}\left[\frac{2n}{(n+m)}\right]$,

$W_m^+ = \mu_\perp \gamma_m + i\chi_{ma} ctg \chi_{ma}\frac{h}{2}, W_m^- = \mu_\perp \gamma_m - i\chi_{ma} tg \chi_{ma}\frac{h}{2}.$

As shown in (Islamov *et al.*, 2021; 2022; Altufaili *et al.*, 2022), the system of linear algebraic equations can be solved analytically using the developed method based on the Cauchy integral and the Lagrange interpolation formula (Raheem *et al.*, 2020; Abdulhameed *et al.*, 2018). As a result of its application, the functional series in (6) are summed up and are expressed through one of the unknown coefficients. As a result, the infinite coupled system of equations is reduced to two algebraic equations for the coefficients $X_n^{\pm}$

$$W_m^+ X_m^- - i\frac{\mu_a}{\mu}\left(\frac{\pi m}{a}\right) X_m^+ = \mu_\perp \gamma_p e^{-i\gamma_p \frac{h}{2}} \delta_{mp,} \tag{7}$$

$$-i\frac{\mu_a}{\mu}\left(\frac{\pi m}{a}\right) X_m^- + W_m^- X_m^+ = \mu_\perp \gamma_p e^{-i\gamma_p \frac{h}{2}} \delta. \tag{8}$$

The solution of the resulting system is in analytical form, namely:

$$X_m^+ = \mu_\perp \gamma_p e^{-i\gamma_p \frac{h}{2}} \delta_{mp,}\left(W_m^+ + i\frac{\mu_a}{\mu}\left(\frac{\pi m}{a}\right)\right)\left\{W_m^+ W_m^- + \left[\frac{\mu_a}{\mu}\left(\frac{\pi m}{a}\right)\right]^2\right\}^{-1}, \tag{9}$$

$$X_m^- = \mu_\perp \gamma_p e^{-i\gamma_p \frac{h}{2}} \delta_{mp,}\left(W_m^- + i\frac{\mu_a}{\mu}\left(\frac{\pi m}{a}\right)\right)\left\{W_m^+ W_m^- + \left[\frac{\mu_a}{\mu}\left(\frac{\pi m}{a}\right)\right]^2\right\}^{-1}. \tag{10}$$

The equality to zero of the determinant of the system of equations (7), (8) determines the dispersion equation for finding the eigen modes of the ferrite resonator, which takes the following form:

$$\left(\mu_{\perp}\gamma_m + i\chi_{ma} ctg\chi_{ma}\frac{h}{2}\right)\left(\mu_{\perp}\gamma_m - i\chi_{ma} tg\chi_{ma}\frac{h}{2}\right) + \left[\frac{\mu_a}{\mu}\left(\frac{\pi m}{a}\right)\right]^2. \tag{11}$$

The unknown coefficients of reflection and transmission in the expressions for the fields (2)-(4) are found through the coefficients $X_m^{\pm}$ (9), (10) by simple recalculation formulas

$$R_m = \left(X_m^+ + X_m^-\right)e^{-i\gamma_m\frac{h}{2}} + \delta_{mp}e^{-i\gamma_m h}, \tag{12}$$

$$T_m = \left(X_m^+ - X_m^-\right)e^{-i\gamma_m\frac{h}{2}}. \tag{13}$$

Let us proceed to the analysis of the natural and forced modes of the ferrite resonator.

3. Analysis of results

Let First, we will consider free vibrations in a ferrite resonator in the absence of an incident waveguide wave. Let us analyze the obtained dispersion equation (11).

An analysis of the dispersion equation shows that in the absence of gyrotropy $(\mu_a = 0)$, dispersion equation (11) splits into two independent equations $\left(\mu_{\perp}\gamma_m + i\chi_{ma} ctg\chi_{ma}\frac{h}{2}\right) = 0, \left(\mu_{\perp}\gamma_m - i\chi_{ma} tg\chi_{ma}\frac{h}{2}\right) = 0,$ which determine, in one case, symmetric, and in the other, asymmetric vibrations over the thickness of the plate *h* made of a magneto-dielectric. It is clear that the number of dispersion curves for each integer oscillation index m will depend on the value of $\chi_{ma}\frac{h}{2}$. In the presence of gyrotropy $(\mu_a \neq 0)$, the vibrations in the ferrite resonator are coupled and there is no separation of vibrations into symmetric and asymmetric vibrations for any index *m*. Depending on the material parameters of ferrite, plate thickness *h*, and waveguide width *a*, for each specific vibration index *m*, several modes of existence of free vibrations should be distinguished.

Let us consider the case when the value of the transverse wave number in an empty waveguide γ_m is a purely imaginary number, i.e. $(\gamma_m)^2 = k^2 - \left(\frac{\pi m}{a}\right)^2 \leq 0.$ This case corresponds to the transcendental regime - the wave amplitude decays exponentially into the depth of the empty waveguide. However, in the region of the ferrite plate, two cases can be realized: the regime of bulk locked modes and the regime of surface modes. Bulk locked modes can exist in the case when the transverse wavenumber in the region of the ferrite plate χ_{ma} is a real value, i.e. for the selected index *m*, the value χ_{ma} satisfies condition $(\chi_{ma})^2 = k^2\varepsilon\mu_{\perp} - \left(\frac{\pi m}{a}\right)^2 \geq 0.$ Surface modes are realized under the opposite condition $(\chi_{ma})^2 = k^2\varepsilon\mu_{\perp} - \left(\frac{\pi m}{a}\right)^2 \leq 0.$ For negative values of the effective permeability of the ferrite layer $\mu_\perp \le 0,$ the transverse wavenumber χ_{ma} is purely imaginary for any vibration index *m*, and therefore, for such values of $\mu_\perp$, the surface regime is always realized, i.e. $(\chi_{ma})^2 \le 0.$ If two conditions

$$(\gamma_m)^2 = k^2 - \left(\frac{\pi m}{a}\right)^2 \le 0, \ (\chi_{ma})^2 = k^2 \varepsilon \mu_\perp - \left(\frac{\pi m}{a}\right)^2 \le 0,$$

are satisfied simultaneously, then the field amplitudes in the two regions decay exponentially from the interface between the media. Such surface modes can be identified with magnon-polariton surface vibrations (Islamov et al., 2018) characteristic of the case when the effective magnetic permeability of the medium $\mu_\perp$ is negative. In this case, such oscillations are possible not only with negative values of the parameter $\mu_\perp$, but also with its positive values, when condition $k^2 \varepsilon \mu_\perp - \left(\frac{\pi m}{a}\right)^2 \le 0$ is satisfied and the transverse wavenumber χ_{ma} is an imaginary value. All roots of the initial dispersion equation (11) for which this condition is satisfied will correspond to magnon-polariton surface vibrations.

In Figure 2 shows the dispersion characteristics (the dependence of the frequency parameter β on the magnetic permeability of ferrite μ_a $\beta = f(\mu_a)$) for the fundamental vibration $m = 1$ with the following values of the material parameters $\varepsilon = 7; \mu = 0{,}7; \theta = \frac{a}{b} = 0{,}8.$ The values of quantities β and μ_a, that are inside this region correspond to the mode of existence of magnon-polariton surface modes in the ferrite plate. Outside this region, bulk vibrations are observed in the ferrite plate. Their spatial distribution depends on the gyrotropy parameter μ_a. The dispersion curve located in the selected shaded area and below the straight line $\beta = 0{,}5$ (dashed line), corresponds to surface vibrations in an empty waveguide. The regime of bulk modes and surface modes are separated by the intersection point of the envelope of the selected region $k^2 \varepsilon \mu_\perp - \left(\frac{\pi m}{a}\right)^2 = 0$ and the dispersion curve (curve 1). The dashed straight line $\beta = 0{,}5$ divides the parameter area into two areas. In the range of parameter values below this line, the regime of surface vibrations is realized from the side of the empty waveguide and the regime of bulk (locked modes) or surface modes inside the ferrite plate. In this case, the roots of the dispersion equation (11) are real. Above this straight line, the roots of the dispersion equation (11) are complex. Figure 2 shows only real values of the complex roots of the dispersion equation. If the parameters of the problem are as follows, then the condition $\beta \ge 0{,}5$ is satisfied, then the mode of forced oscillations can be realized at excitation of a ferrite plate by the fundamental waveguide wave. For this case, the modules of the transmission coefficient $|T_1|$ and the reflection coefficient $|R_1|$ were calculated depending on the frequency parameter β for the given values of $\varepsilon = 7; \mu = 0{,}7; \mu_a = 0{,}5; \theta = \frac{a}{b} = 0{,}8.$ The calculation results are shown in Figure 3.

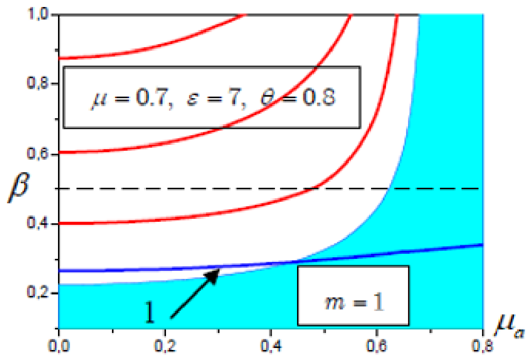

Fig. 2. Frequency dependence parameter β on the value μ_a

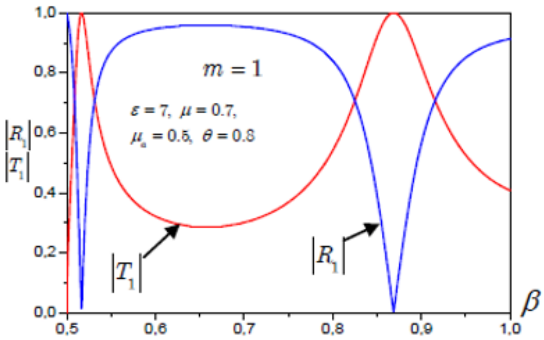

Fig. 3. Dependence of the moduli of the transmission coefficients $|T_1|$ and reflection $|R_1|$ on the frequency parameter β.

The distance on the frequency scale between resonances is close to half-wave resonance in a gyrotropic medium of a ferrite plate. It should be noted that the reflection coefficient $|R_1|$ does not reach its maximum value equal to 1, in contrast to the transmission coefficient, which reaches this value at resonant frequency values. By varying the magnitude of the transverse magnetic field, it is possible to change the effective magnetic permeability of the ferrite and, according to the dispersion characteristics (Figure 2), the resonant frequency of the forced vibrations will change. This leads to the possibility of electrical frequency tuning, at which full passage of the waveguide wave is observed.

The direction of the zero of the radiation patterns $\varphi_{\min}$ will be changed. The optimality criterion is the maximization of the ratio of the coefficient of directional action in the direction $\varphi_{\max}$ to coefficient of directional action at the minimum $\varphi_{\min}$. Figure 4 shows the radiation patterns corresponding to the amplitude-phase distribution. For an antenna array with more than 5 radiating elements, we use the code for the genetic algorithm from (Islamov et al., 2022) instead of the particle swarm method.

On Figure 4 shows radiation diagrams corresponding to the amplitude-phase distribution, let us form at a frequency of 2,7 *GHz* the total radiation pattern with the maximum directivity in the direction $\vartheta = 45^o$, $\varphi = -150^o$; this radiation pattern is shown in Figure 5.

Figure 6, shows the radiation pattern in the plane of the screen. Further, in addition to the maximum directivity coefficient in the direction $\vartheta = 45^o$, $\varphi = -150^o$, we require zero in the radiation patterns in the plane of the screen (ϑ = 90°, φ = – 90°). We will, as before, maximize the ratio of the coefficient of directional action. The results are shown in Figure 6. The maximum of the directivity factor, equal to 9,5 *dB*, is shifted and obtained in the direction ϑ_{max} = 51°, φ_{max} = – 140°.

There is no need to allocate space for a pre-designed antenna array with any known regular structure.

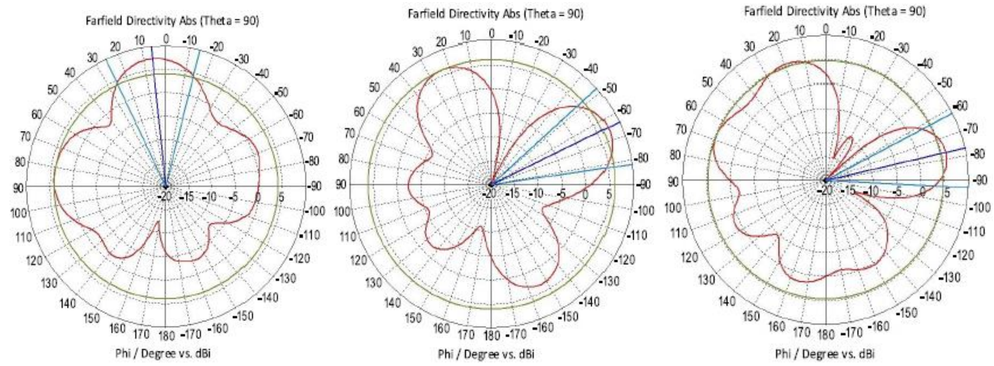

a) b) c)

Fig. 4. Radiation patterns correspond to the amplitude-phase distribution: a) zero is not generated; b) φ_{min} = – 18°; c) φ_{min} = – 45°

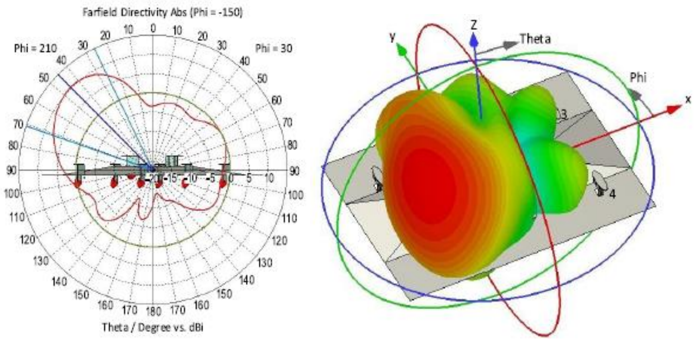

a) b)

Fig. 5. Radiation patterns (a) and 3*D* model (b) at ϑ = 45°, φ = – 150°

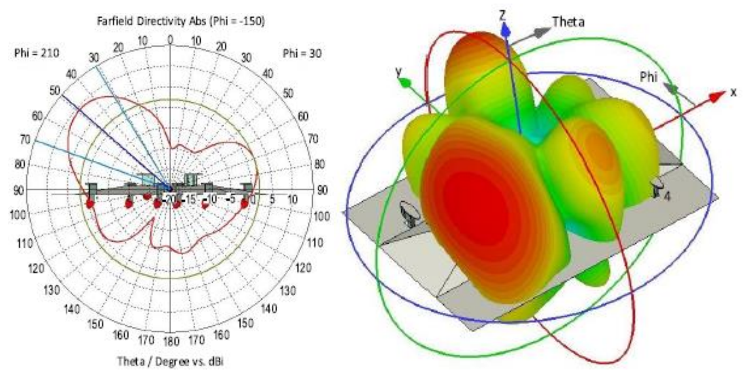

a) b)

Fig. 6. Radiation patterns (a) and 3*D* model (b) at ϑ = 51°, φ = – 140°

Depending on the location of the antenna and the model of external influencing factors, the design of the final product is supplemented with a radio-transparent radome or a radio-transparent shelter. Restrictions are imposed on the structural elements of such structures to protect antenna arrays due to the fact that partial radiation patterns must experience minimal and identical distortions. The proposed method allows for removing a number of limitations. For example, fairings can be of arbitrary shape and complemented by asymmetrical stiffeners.

4. Conclusion

In this work, the simulation of the electromagnetic field of the microwave waveguide is carried out, taking into account the anisotropy of the medium. A dispersion equation and expressions for the reflection and transmission coefficients of a waveguide wave are obtained. 3*D* radiation patterns of the microwave range waveguide are plotted taking into account the gyrotropy of the medium. On the basis of the developed new method, an explicit analytical solution of the boundary value problem of natural and forced oscillations of a ferrite resonator in a microwave rectangular waveguide with a transverse magnetic field is found. Various modes of excitation of bulk and surface self-oscillations in a ferrite resonator are analyzed.

The results obtained in the work can be used to create new microwave devices for transmitting and receiving signals. And also the results obtained can be used to create polarizers, filters and polarization-sensitive waveguide switches. Based on the results obtained, it is possible to form planar active antennas, in which the activation of layers of a composite metamaterial leads to the appearance of new resonant frequencies, which makes it possible to form a multiband printed antenna with controllable ranges, since initially printed antennas have a narrow operating frequency range.

References

Kerim, G., Suad, B. (2015). A quantized water cycle optimization algorithm for antenna array synthesis by using digital phase shifters. *International Journal of RF and Microwave Computer-Aided Engineering*, *25*(1), 21-29.

Taisir, H.I., Zoubir, M.H. (2010). Array pattern synthesis using digital phase control by quantized particle swarm optimization. *IEEE Transactions on Antennas and Propagation*, *58*(6), 2142-2145.

Wang, Z., Song, Y., Mu, T. & Ahmad, Z. (2018). A short-range range-angle dependent beampattern synthesis by frequency diverse array. *IEEE Access*, 6, 22664-22669.

Lima, A.M., de Freitas, J.V. & Lavor, O.P. (2021). Analysis of the Resonator Element in Different Positions in the Circular Patch Microstrip Antenna. *Journal of Microwaves, Optoelectronics and Electromagnetic Applications*, *20*(1), 16-29.

Lima, A.M., Cunha, N.H.O. & da Silva, J.P. (2020). Effect of metamaterial cells array on a microstrip patch antenna design. *Journal of Microwaves, Optoelectronics and Electromagnetic Applications*, *19*(3), 327-342.

Li, J., Ren, S. & Guo, C. (2020). Synthesis of Sparse Arrays Based on CIGA (Convex Improved Genetic Algorithm). *Journal of Microwaves, Optoelectronics and Electromagnetic Applications*, *19*(4), 444-456.

Liang, S., Feng, T. & Sun, G. (2017). Sidelobe-level suppression for linear and circular antenna arrays via the cuckoo search-chicken swarm optimisation algorithm. *IET Microwaves, Antennas Propagation*, 11, 209-218.

Singh, H., Mittal, N., Singh, U. & Salgotra, R. (2022). Synthesis of non-uniform circular antenna array for low side lobe level and high directivity using self-adaptive Cuckoo search algorithm. *Arabian Journal for Science and Engineering*, 47, 3105-3118.

Yang, G., Zhang, Y. & Zhang, S. (2021). Wide-band and wide-angle scanning phased array antenna for mobile communication system. *IEEE Open Journal of Antennas and Propagation*, 2, 203-212.

Wang, R.Q., Jiao, Y.C. (2019). Synthesis of wideband rotationally symmetric sparse circular arrays with multiple constraints. *IEEE Antennas and Wireless Propagation Letters,* 18, 821-825.

Hui, L., Yikai, C. & Ulrich, J. (2022). Synthesis, Control, and Excitation of Characteristic Modes for Platform-Integrated Antenna Designs: A design philosophy. *IEEE Antennas and Propagation M*agazine, *64*(2), 41-48.

Castillo, R., Ma, R. & Behdad, N. (2021). Platform-based electrically-small HF antenna with switchable directional radiation patterns. *IEEE Transactions on Antennas and Propagation*, *69*(8), 4370-4379.

Liu, Y., Zhang, J., Ren, A., Wang, H. & Sim, C. (2019). TCM-based heptaband antenna with small clearance for metal-rimmed mobile phone applications. *IEEE Antennas and Wireless Propagation Letters*, *18*(4), 717-721.

Islamov, I.J., Ismibayli, E.G., Gaziyev, Y.G., Ahmadova, S.R. & Abdullayev, R.Sh. (2019). Modeling of the electromagnetic feld of a rectangular waveguide with side holes. *Progress in Electromagnetics Research*, 81, 127-132.

Islamov, I.J., Ismibayli, E.G. (2018). Experimental study of characteristics of microwave devices transition from rectangular waveguide to the megaphone. *IFAC-Papers OnLine*, *51*(30), 477-479.

Ismibayli, E.G., Islamov, I.J. (2018). New approach to definition of potential of the electric field created by set distribution in space of electric charges. *IFAC-Papers OnLine*, *51*(30), 410-414.

Islamov, I.J., Ismibayli, E.G., Hasanov, M.H., Gaziyev, Y.G., Ahmadova, S.R. & Abdullayev, R.Sh. (2019). Calculation of the electromagnetic field of a rectangular waveguide with chiral medium. *Progress in Electromagnetics Research*, 84, 97-114.

Islamov, I.J., Hunbataliyev, E.Z. & Zulfugarli, A.E. (2022). Numerical simulation of characteristics of propagation of symmetric waves in microwave circular shielded waveguide with a radially inhomogeneous dielectric filling. *International Journal of Microwave and Wireless Technologies*, *14*(6), 761-767.

Islamov, I.J., Hasanov, M.H. & Abbasov, M.H. (2021). Simulation of electrodynamic processes in a cylindrical-rectangular microwave waveguide systems transmitting information, *International Conference on Theory and Application of Soft Computing, Computing with Words, Perception and Artificial Intelligence*, 246-253.

Islamov, I., Humbataliyev, E. (2022). General approaches to solving problems of analysis and synthesis of directional properties of antenna arrays. *Advanced Electromagnetics*, *11*(4), 22-33.

Altufaili, M.M.S., Najaf, A.N. & Idan, Z.S. (2022). Design of circular-shaped microstrip patch antenna for 5G applications. *Telecommunication, Computing, Electronics and Control*, *20*(1), 19-26.

Raheem, N. & Qasem, N. (2020). A compact multi-band notched characteristics UWB microstrip patch antenna with a single sheet of graphene. *Telecommunication, Computing, Electronics and Control*, *18*(4), 1708-1818.

Abdulhameed, M.K., Mohamad Isa, M.S., Zakaria, Z. & Mohsin, M.K. (2018). Controlling the radiation pattern of patch antenna using switchable EBG. *Telecommunication, Computing, Electronics and Control*, *16*(5), 2014-2022.